


 Cite this: *RSC Adv.*, 2018, **8**, 12752

Synthesis and self-assembly of a novel amphiphilic diblock copolymer consisting of isotactic polystyrene and 1,4-trans-polybutadiene-graft-poly(ethylene oxide)

 HuaQing Liang,^a QiHua Zhou,^a YongJiang Long,^a WanChu Wei,^a Shuo Feng,^a GuoDong Liang^{ID,ab} and FangMing Zhu^{ID,*ab}

Herein, a novel amphiphilic diblock copolymer consisting of isotactic polystyrene (*iPS*) and 1,4-*trans*-polybutadiene-*graft*-poly(ethylene oxide) (1,4-*trans*-PBD-*g*-PEO), *iPS-b-(1,4-*trans*-PBD-*g*-PEO)*, was synthesized by the combination of living coordination copolymerization and graft copolymerization. *iPS-b-1,4-*trans*-PBD* was firstly synthesized *via* sequential monomer addition in the presence of 1,4-dithiabutandiyli-2,2'-bis(6-cumenyl-4-methylphenoxy) titanium dichloride (complex 1) activated by triisobutyl aluminum modified methylaluminoxane (MMAO). Moreover, hydroboration of double bonds in the 1,4-*trans*-PBD blocks were performed with 9-borabicyclo[3.3.1]nonane (9-BBN) and subsequent oxidation by NaOH/H₂O₂ to form hydroxyls. Consequently, PEO was grafted into the hydroxylated 1,4-*trans*-PBD block in terms of ring-opening polymerization of ethylene oxide with potassium/naphthalide as initiator. We also described solvent-evaporation-induced self-assembly of *iPS-b-1,4-*trans*-PBD* in *n*-dodecane and *iPS-b-1,4-*trans*-PBD-g-PEO* in aqueous solution, which were selective solvent for 1,4-*trans*-PBD and for 1,4-*trans*-PBD-*g*-PEO blocks, respectively. In these cases, tetrahydrofuran (THF) was used as good and volatile solvent. These resultant *iPS*-containing diblock copolymers could self-assemble into spherical nano-micelles with an *iPS* core as amorphous agglomeration or a very low degree of crystallinity resulting from slow crystallization rate and nanoconfinement. In addition, after isothermal crystallization of *iPS* in the micellar cores self-assembled in *n*-dodecane at 120 °C for 3 hours, the micellar morphology changed from sphere-like to platelet-like. It was believed that isothermal crystallization of *iPS* induced the deformation of the micelles.

Received 9th February 2018
 Accepted 29th March 2018

DOI: 10.1039/c8ra01288a
rsc.li/rsc-advances

Introduction

Isotactic polystyrene (*iPS*) is an important stereoregular polymer with a good application foreground because of its unique physical and chemical properties such as high melting temperature, high heat deflection temperature and good corrosion resistance. *iPS* was first synthesized by the Ziegler-Natta catalyst in the 1950s with coordination polymerization. However, the living stereospecific living polymerization of styrene and 1,3-butadiene were achieved in 2010 by titanium complexes containing a tetradentate [OSO]-type bis(phenolato) ligand ([OSO]-Ti) and the polymerisates were respectively *iPS* and 1,4-*trans*-polybutadiene (1,4-*trans*-PBD) with narrow molecular weight distribution. Furthermore, the diblock copolymer consisting of *iPS* and 1,4-*trans*-PBD was synthesized

by this [OSO]-Ti complex *via* sequential monomer addition,¹ which makes it possible for the research into the self-assembly of *iPS*-core diblock copolymers in selective solvent.²

The self-assembly of crystalline-coil diblock copolymers has drawn general attention at recent years because of their remarkable advantages.³⁻¹⁰ The insoluble crystalline block undergoes microphase separation and aggregation to form the core of micelle-like objects, surrounded by a solvent-swollen corona that provides colloidal stability. Crystalline-coil diblock copolymers can enrich the nano structures of the micelles as some complex architectures may be obtained by controlling the crystallization pathway.¹¹⁻¹³ There are several strategies for the crystallization-driven self-assembly of the crystalline-coil block copolymers, that are, thermally controlled crystallization,¹⁴ morphological transitions,¹⁵ hierarchical assembly,¹⁶ and “living” crystallization.¹⁷ In most cases, the crystalline-coil diblock copolymers contain a crystalline core-forming block such as polyethylene (PE),¹⁸⁻²⁰ isotactic (*iPP*) or syndiotactic polypropylene (*sPP*),^{21,22} poly(ferrocenyldimethylsilane) (PFDSMS),²³⁻²⁵ polyethylene oxide (PEO),²⁶⁻²⁸ poly(L-lactide)

^aGDHPPC Lab, School of Chemistry, Sun Yat-Sen University, 510275, China. E-mail: cesfm@mail.sysu.edu.cn; Fax: +86-20-84114033; Tel: +86-20-84113250

^bKey Lab for Polymer Composite and Functional Materials of Ministry of Education, School of Chemistry, Sun Yat-Sen University, Guangzhou, 510275, China



(PLLA) or poly(D-lactide) (PDLA),^{29,30} poly(ϵ -caprolactone) (PCL),³¹⁻³⁵ polythiophene (PTh),^{36,37} polyacrylonitrile (PAN).^{38,39} *iPS* was considered as a semi-crystalline polymer characterized by slow crystallization rates and low crystallinity.⁴⁰⁻⁴² Therefore, the solution crystallization and self-assembly of *iPS*-core block copolymers in selective solvent have caused great interest.⁴³

Recently, we have reported the self-assembly of *iPS*-*b*-PEO in *N,N*-dimethylformamide (DMF) with *iPS* as core.² To the best of our knowledge, there is no example for the investigation of the self-assembly of *iPS*-*b*-1,4-*trans*-PBD in the nonpolar solvent such as *n*-heptane or *n*-dodecane.

Note that there are a lot of double bonds in the PBD block of the PBD-containing diblock copolymers, which is easy to be hydroxylated. After hydroxylation, the hydroxyl connected to the backbone can initiate the ring-opening polymerization of ethylene oxide using the initiator of naphthalene/potassium to form new diblock copolymers. Undoubtedly, the graft of poly(ethylene oxide) (PEO) can change the polarity of the PBD block and makes it possible to self-assemble in the polar solvent such as water. In this article, the catalytic system [OSO₂]Ti/isobutyl modified methylaluminoxane (MMAO) was used to synthesize the diblock copolymers containing isotactic polystyrene segment and *trans*-1,4-polybutadiene segment. Furthermore, the *iPS*-*b*-1,4-*trans*-PBD-*g*-PEO was synthesized and characterized. The self-assembly behaviors of *iPS*-*b*-1,4-*trans*-PBD in *n*-dodecane and *iPS*-*b*-1,4-*trans*-PBD-*g*-PEO in aqueous solution were explored.

Experimental

Materials

All reagents were purchased from Aladdin and J&K Scientific. Styrene was dried with calcium hydride and distilled on a vacuum line. 1,3-butadiene was dried with calcium hydride at -40°C and distilled at room temperature to form a toluene solution. Tetrahydrofuran (THF) was dried by distilling from potassium with benzophenone as an indicator. Toluene was dried by distilling from sodium with benzophenone as an indicator. 9-Borabicyclo[3.3.1]nonane (9-BBN) (Aladdin, 0.5 M in THF) was used as received. NaOH and H₂O₂ (30 wt%) were used as received. Naphthalene/potassium was prepared using dry THF, naphthalene (Aladdin, $\geq 99\%$), and excess potassium metal. Ethylene oxide (EO) was distilled and collected on the vacuum line and kept as a liquid at -34°C . 1.9 M solution of triisobutyl aluminum modified methylaluminoxane (MMAO) in heptane was used as received.

Synthesis of isotactic polystyrene-block-1,4-*trans*-polybutadiene (*iPS*-*b*-1,4-*trans*-PBD). The *iPS*-*b*-1,4-*trans*-PBD was synthesized as literature.¹ A typical example was as follows. A 100 mL flask equipped with a magnetic bar was charged with 6.3 mL of a 1.9 M solution of MMAO in *n*-heptane, 8.7 mL toluene, and 5.0 mL of a solution of 10 μmol [OSO₂]Ti complex in toluene. The mixture was stirred for 5 min at room temperature. The polymerization was started by injecting 0.7 mL styrene. After 2 h, 4.6 mL of a 4.3 M solution of 1,3-butadiene in toluene was then rapidly added to this flask. The copolymerization continuously proceeded for an additional 2 h. The

reaction mixture was terminated by introducing 2 mL ethanol containing the antioxidant. The polymer was precipitated in 200 mL ethanol acidified with 20 mL concentrated hydrochloric acid, recovered by filtration, washed with an excess of ethanol, and dried to constant weight under vacuum at room temperature.

Preparation of isotactic polystyrene-block-hydroxylated 1,4-*trans*-polybutadiene. The hydroboration of *iPS*-*b*-1,4-*trans*-PBD was performed in a Schlenk flask equipped with a condenser. *iPS*-*b*-1,4-*trans*-PBD was dissolved in dry THF and then 9-BBN was added dropwise at room temperature. After hydroboration at 75°C for 48 h, the reaction solution was cooled to 0°C . The required amount of 6 M NaOH (aq.) and then 30 wt% H₂O₂ (aq.) was added dropwise. After oxidation at 50°C for 24 h, the *iPS*-*b*-hydroxylated 1,4-*trans*-PBD was precipitated into water and filtered. The resultant polymer was washed with methanol for several times to remove traces of boric acid.

Preparation of isotactic polystyrene-block-(1,4-*trans*-polybutadiene-*graft*-poly(ethylene oxide)) (*iPS*-*b*-(1,4-*trans*-PBD-*g*-PEO)). *iPS*-*b*-(1,4-*trans*-PBD-*g*-PEO) was prepared by ring-opening graft copolymerization of ethylene oxide on hydroxylated 1,4-*trans*-PBD block initiated by naphthalene/potassium. The *iPS*-*b*-1,4-*trans*-PBD and dry THF was placed in a Schlenk flask at room temperature. Graft copolymerization of ethylene oxide was initiated by a dark green THF solution of naphthalene/potassium at -40°C for 5 min. Heating temperature to 25°C , the reaction was carried out for more than 24 h until the solution turned to light yellow. The copolymerization solution was quenched with concentrated hydrochloric acid acidic methanol, and then the polymer was precipitated in diethyl ether. After isolation by filtration, the polymer was purified by removing poly(ethylene oxide) homopolymer through dialyzed against deionized water. The insoluble fraction of the *iPS*-*b*-(1,4-*trans*-PBD-*g*-PEO) was dried under vacuum.

The self-assembly of *iPS*-*b*-1,4-*trans*-PBD in *n*-dodecane. 1,4-*trans*-PBD can rapidly dissolve in *n*-dodecane after slightly heated, while *iPS* can not dissolve in *n*-dodecane after heated to 150°C , which demonstrate that *n*-dodecane is a selective solvent for *iPS*-*b*-1,4-*trans*-PBD. Moreover, tetrahydrofuran (THF) is a good solvent for both *iPS* and 1,4-*trans*-PBD. The solvent-induced self-assembly of *iPS*-*b*-1,4-*trans*-PBD can be generally proceeding as follows. Taking the preparation of self-assembled solution of 0.5 mg mL⁻¹ for example, 5.0 mg of *iPS*-*b*-1,4-*trans*-PBD was dissolved in about 2 mL THF and the solution was added to 10 mL *n*-dodecane dropwise to obtain a light blue solution indicating the self-assembly of *iPS*-*b*-1,4-*trans*-PBD in *n*-dodecane. Then the THF was completely removed by vacuum evaporation for several hours proved by ¹H NMR.

The self-assembly of *iPS*-*b*-(1,4-*trans*-PBD-*g*-PEO) in aqueous solution. Water is a suitable selective solvent for the self-assembly of *iPS*-*b*-(PBD-*g*-PEO). The solvent-induced self-assembly of *iPS*-*b*-(PBD-*g*-PEO) is generally proceeding as follows. 5.0 mg of *iPS*-*b*-(1,4-*trans*-PBD-*g*-PEO) was dissolved in about 2 mL of THF and the solution was added to 10 mL of deionized water to obtain a light blue solution, implying the self-assembly of *iPS*-*b*-(1,4-*trans*-PBD-*g*-PEO) in aqueous



solution. Then the THF was completely removed by dialyzed against deionized water for a week proved by ^1H NMR.

Measurements

^1H NMR (400 MHz) and ^{13}C NMR (100 MHz) spectra were recorded in CDCl_3 at 25 °C on a Varian Unity Inova 400 spectrometer. Molecular weight and molecular weight distribution (M_w/M_n) were determined by gel permeation chromatography (GPC) against narrow molecular weight distribution polystyrene standards on a Waters 2414 refractive index detector at 40 °C with THF as the eluent.

The morphology of the micelles was observed by scanning electron microscope (SEM) (Hitachi S-4800) with an accelerating voltage of 10.0 kV and transmission electron microscope (TEM) (JEM 1400Plus) with an accelerating voltage of 120 kV. For the SEM observation, a drop from the previously prepared micellar solution was deposited onto a mica plate. The mica plate was dried at room temperature for 12 hours before examination by SEM. For the TEM observation, a drop from the previously prepared micellar solution was deposited onto a carbon-coated copper grid.

Dynamic light scattering (DLS) measurements were conducted on a Brookhaven BI-200SM apparatus with a BI-9000AT digital correlator and a He-Ne laser at 632 nm. Data were analyzed by the CONTIN algorithm, while the average hydrodynamic diameter (D_h) and size polydispersity of the particles were obtained by a cumulant analysis of the experimental correlation function.

DSC experiments were carried out on a TA Instruments (New Castle, DE, USA) Q10 calorimeter. Calibration was performed

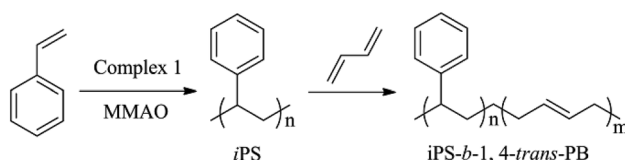
with indium and tin, and all tests were run employing ultrapure nitrogen as the purge gas. DSC heating and cooling scans were performed at 10 °C min $^{-1}$ over the temperature range 0 °C to 250 °C for standard measurements.

Results and discussion

Synthesis and characterization of *iPS*-Containing diblock copolymers

In recent years, [OSO]-based titanium complexes have attracted much attention because of the isospecific polymerization of styrene and α -olefins.^{1,44,45} In 2003, Okuda *et al.*⁴⁴ first reported that [OSO]-Ti complexes could promote polymerization of styrene upon activation with methylalumininoxane (MAO) to give *iPS*.^{46–48} Subsequently, the living stereospecific polymerization of styrene and 1,3-butadiene catalyzed by 1,4-dithiabutandiyli-2,2'-bis(6-cumenyl-4-methylphenoxy) titanium dichloride (complex 1) activated with MAO was reported by Capacchione in 2010.¹ In this case, we synthesized the diblock copolymers of *iPS*-*b*-1,4-*trans*-PBD with complex 1 and MMAO used as cocatalyst *via* sequential monomer addition as shown in Scheme 1 and Table 1.

Moreover, the resultant diblock copolymers were characterized by GPC, NMR and DSC. The ^1H NMR and ^{13}C NMR (Fig. 1 and 2) shows that the PS block is *iPS* ($mmm \geq 95\%$) and the PBD block is 1,4-*trans*-PBD (1,4-*trans* addition $\geq 95\%$). In addition, the relative length of the *iPS* block and the 1,4-*trans*-PBD block could be calculated from the ^1H NMR. To study the thermal properties, one of the prepared diblock copolymers of *iPS*-*b*-1,4-*trans*-PBD with no other heat treatment or mechanical treatment was used for DSC scan at a heating rate of 10 °C min $^{-1}$ (the first heating curve for solution crystallization, as shown in Fig. 3a), which exhibits that the melting temperature (T_m) of *iPS* block ($M_n = 9.2 \times 10^4$) is 220 °C and 1,4-*trans*-PBD block ($M_n = 2.9 \times 10^4$) is 45 °C/82 °C, indicating these two blocks were crystalline. After cooling at a rate of 10 °C min $^{-1}$, this copolymer was heating again at a rate of 10 °C min $^{-1}$ (the second heating curve, as shown in Fig. 3b). In this case, the area of crystal-melting peak of *iPS* at 220 °C was much smaller than that in the first heating curve, suggesting the very slow crystallization rate of *iPS*. To confirm this, the third heating



Scheme 1 The synthesis of *iPS*-*b*-1,4-*trans*-PBD by complex 1/MMAO *via* sequential monomer addition.

Table 1 Block copolymerization of styrene with 1,3-butadiene catalyzed by complex 1/MMAO *via* sequential monomer addition^a

Entry	St/BD in feed (mmol mmol $^{-1}$)	C_{PBD}^b (%)	C_{trans}^c (%)	$M_n^d \times 10^{-4}$	M_w/M_n^d	T_{mPS} (°C) e
1	0/8.0	100	95	4.6	1.30	—
2	1.3/8.0	78.7	96	7.0	1.36	222
3	2.0/8.0	71.4	96	7.9	1.39	220
4	3.4/8.0	57.1	96	10.0	1.30	222
5	8.0/18.7	54.1	95	15.8	1.27	220
6	8.0/8.0	39.1	95	14.6	1.20	220
7	8.0/3.4	28.8	97	13.1	1.25	221
8	8.0/0	0	—	11.3	1.20	221

^a Polymerization conditions: Ti = 1.0 μmol ; [Al]/[Ti] = 1200; $T = 25$ °C; $V_{\text{tot}} = 20$ mL (styrene + toluene); polymerization time, 2 h (styrene) + 2 h (butadiene). ^b PBD content in copolymers, determined from ^1H NMR spectra. ^c *trans*-1,4-regularities in PBD block, determined from ^1H NMR spectra. ^d Determined by GPC with THF as the eluent. ^e Melting temperature relative to the isotactic polystyrene block in the resulting *iPS*-*b*-1,4-*trans*-PBD, determined by 10 °C min $^{-1}$ heating rate DSC scans.



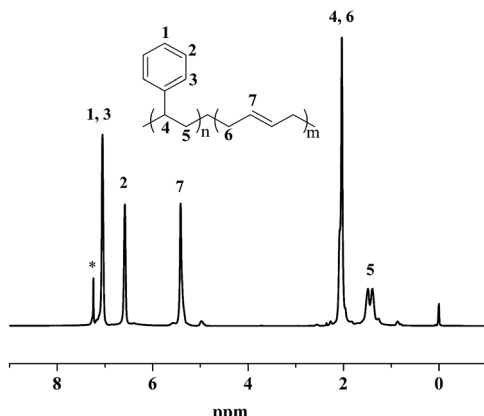


Fig. 1 ^1H NMR spectrum of *i*PS-*b*-1,4-*trans*-PBD (Entry 6 in Table 1) synthesized by complex 1/MMAO via sequential monomer addition.

curve at a rate of $10\text{ }^\circ\text{C min}^{-1}$ as shown in Fig. 3c was displayed after the isothermal crystallization of this sample at $120\text{ }^\circ\text{C}$ for 3 hours. As might be expected, the area of crystal-melting peak of *i*PS at $220\text{ }^\circ\text{C}$ greatly increased, which is even bigger than that in the first heating curve.

The hydroxylation of the 1,4-*trans*-PBD block was carried out as procedures reported.^{49,50} Note that the hydroboration of the 1,4-microstructure of polybutadiene was more difficult than the 1,2-microstructure.⁴⁹ Moreover, as reported by Ramakrishnan,⁵⁰ 83% 1,4-*cis*-polybutadiene synthesized by the ring-opening metathesis polymerization of 1,5-cyclooctadiene can be easily hydroborated at around $60\text{ }^\circ\text{C}$. However, in this case, more than 95% 1,4-*trans*-PBD block in the copolymer can hardly be hydroborated on the same conditions. Therefore, the temperature of hydroboration was raised to $75\text{ }^\circ\text{C}$ and the 1,4-*trans*-PBD block was almost completely hydroxylated. As shown in Fig. 4, the 1,4-*trans*-PBD block was almost completely hydroxylated. Compared with the ^1H NMR spectrum of the 1,4-*trans*-PBD block before hydroxylation, the corresponding peak at 5.44 ppm assigned to the chemical shift of unsaturated bond in 1,4-*trans*-PBD block almost disappears and the characteristic peak at

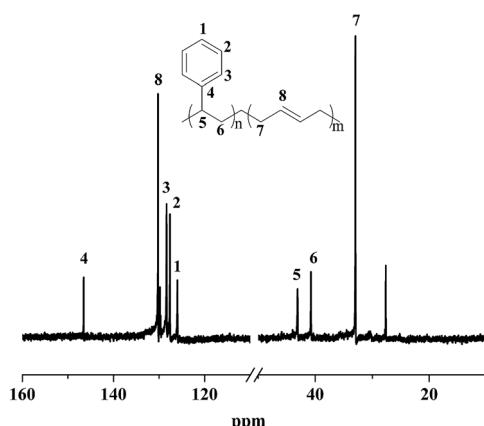


Fig. 2 ^{13}C NMR spectrum of *i*PS-*b*-1,4-*trans*-PBD (Entry 6 in Table 1) synthesized by complex 1/MMAO via sequential monomer addition.

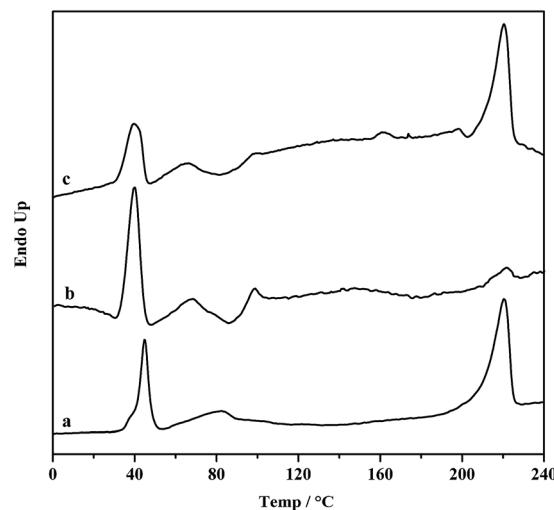


Fig. 3 DSC scans of *i*PS-*b*-1,4-*trans*-PBD with $M_n = 1.21 \times 10^5$ at $10\text{ }^\circ\text{C min}^{-1}$ heating rate, (a) the first heating curve of the newly prepared sample; (b) the second heating curve after cooling at a rate of $10\text{ }^\circ\text{C min}^{-1}$; (c) the third heating curve after isothermal crystallization at $120\text{ }^\circ\text{C}$ for 3 h.

3.52 ppm of the methine proton of CHOH appears after hydroxylation.

The graft of PEO into 1,4-*trans*-PBD block was performed using naphthalene/potassium as initiator *via* anion ring-opening polymerization of ethylene oxide (as shown in Scheme 2). To remove as completely as possible the PEO homopolymer, the graft copolymerization products were dispersed in water by stirring and dialyzed against deionized water with a dialysis bag molecular weight cut off of 50 000 for a week. The GPC results indicated that the PEO homopolymer was almost removed by dialysis against deionized water. Fig. 5 shows a representative ^1H NMR spectrum of *i*PS-*b*-(1,4-*trans*-PBD-*g*-PEO) prepared from Entry 6 in Table 1. The high and

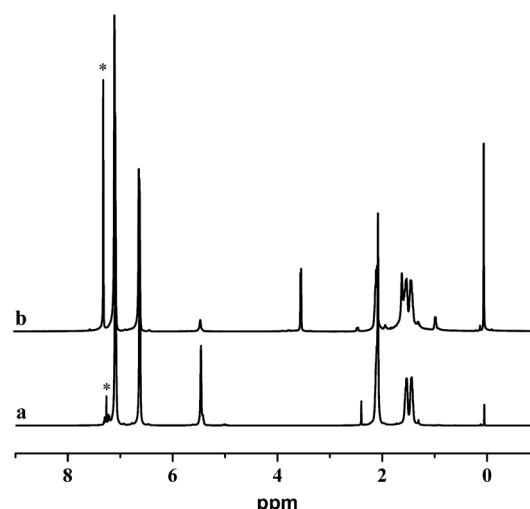


Fig. 4 ^1H NMR spectra of *i*PS-*b*-1,4-*trans*-PBD (Entry 6 in Table 1) before (a) and after (b) hydroxylation.

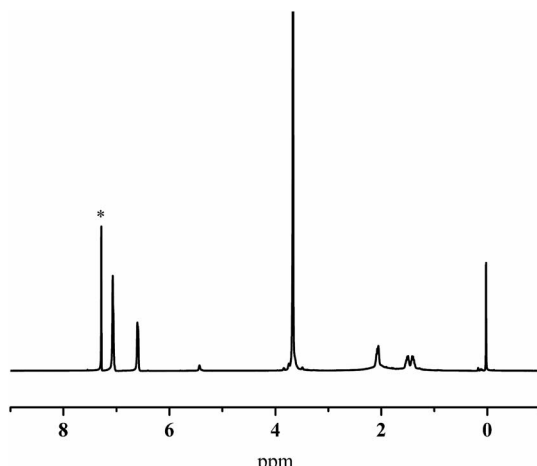
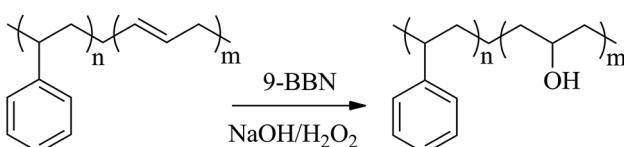


Fig. 5 ¹H NMR spectrum of *iPS-b-(1,4-trans-PBD-g-PEO)* prepared from Entry 6 in Table 1 by graft copolymerization.

shark peak at 3.67 ppm is the characteristic chemical shift of PEO and the characteristic peak of the methine proton of CHOH at 3.52 ppm almost disappears. These results demonstrated that the *iPS-b-(1,4-trans-PBD-g-PEO)* was successfully prepared.

The self-assembly of *iPS-b-1,4-trans-PBD* in *n*-dodecane

The self-assembly of *iPS-b-1,4-trans-PBD* was performed in *n*-dodecane, a selective solvent for 1,4-*trans*-PBD. A solution of the *iPS-b-1,4-trans-PBD* in THF was added dropwise to *n*-dodecane to form a light blue solution, indicating the self-assembly process of the *iPS-b-1,4-trans-PBD* (Entry 6 in Table 1). Then the THF was completely removed by vacuum evaporation. DLS measurement displays that the average hydrodynamic diameter (D_h) of the self-assembled micelles of *iPS-b-1,4-trans-PBD* in *n*-dodecane were around 80 nm as shown in Fig. 6, which is much larger than that of the individual chain in THF (~35 nm), confirming the self-assembling of *iPS-b-1,4-trans-PBD* in *n*-dodecane. Fig. 7 shows the SEM micrographs of the self-assembled micelles of *iPS-b-1,4-trans-PBD* in *n*-dodecane after prepared for 0 day, 7 days and 14 days, respectively. Spherical micelles with a diameter of about 60 nm were observed when the micelles were newly prepared. After prepared for two weeks, the micelles aggregated but keep their morphology to be spherical and identical diameter of about 60 nm, which suggests that the *iPS* core did not crystallize at room temperature as aging. To explain these outcomes, we suppose that the core-forming *iPS* block could not crystallize or have a very low degree of crystallinity in



Scheme 2 The hydroxylation of *iPS-b-1,4-trans-PBD* synthesized by complex 1/MMAO via sequential monomer addition.

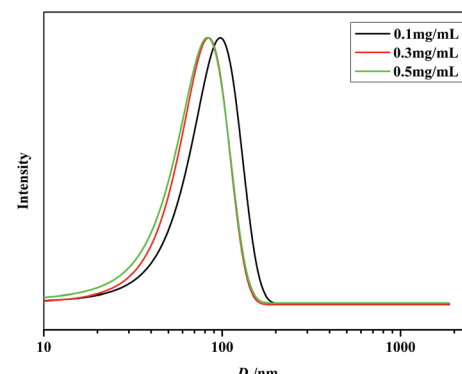


Fig. 6 D_h distributions of the self-assembled micelles of *iPS-b-1,4-trans-PBD* (Entry 6 in Table 1) in *n*-dodecane (0.1 mg mL⁻¹, 0.5 mg mL⁻¹, 1.0 mg mL⁻¹, respectively).

nanoconfined space of micelles when the micelles were newly formed by removing the THF. After aged for a period at room temperature, the core-forming *iPS* block still could not crystallize as a result of the room temperature much lower than the glass transition temperature. The TEM images of self-assembled micelles of *iPS-b-1,4-trans-PBD* (as shown in Fig. 8) in *n*-dodecane also suggested the formation of spherical micelles.

To confirm our speculation, the prepared micellar solution was heated to 120 °C for 3 h to promote the crystallization of the

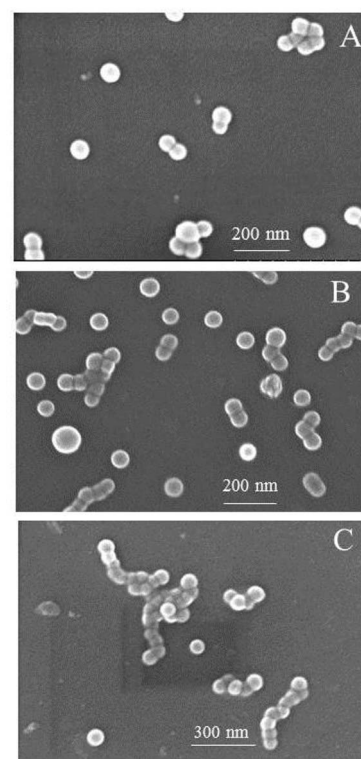


Fig. 7 SEM microscopy of the self-assembled micelles of *iPS-b-1,4-trans-PBD* (Entry 6 in Table 1) in *n*-dodecane after prepared for, respectively, (A). 0 day, (B). 7 day, (C). 14 day.

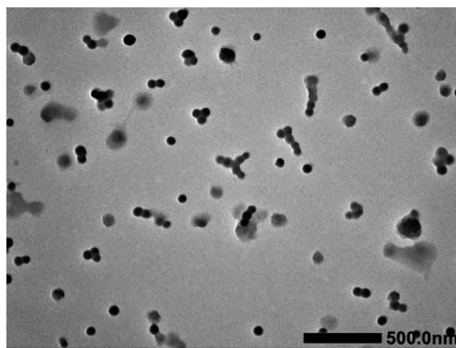


Fig. 8 TEM images of the self-assembled micelles of *iPS-b-(1,4-trans-PBD)* prepared from Entry 6 in Table 1 in *n*-dodecane.

core-forming *iPS* block. Fig. 9 shows the SEM microscopy of the self-assembled micelles of *iPS-b-1,4-trans-PBD* (Entry 6 in Table 1) before and after isothermal crystallization. The micellar morphology changed from sphere-like to platelet-like and the diameter changed larger after isothermal crystallization. The TEM images of the self-assembled micelles before and after isothermal crystallization are exhibited in Fig. 10, which also suggests that the micellar morphology changed from sphere-like to bigger platelet-like induced by the crystallization of the *iPS* core.

The self-assembly of *iPS-b-(1,4-trans-PBD-g-PEO)* in aqueous solution

The self-assembly of *iPS-b-(1,4-trans-PBD-g-PEO)* was performed in aqueous solution, which is a selective solvent for PEO. A solution of the *iPS-b-(1,4-trans-PBD-g-PEO)* in THF was added dropwise to deionized water to form a light blue solution,

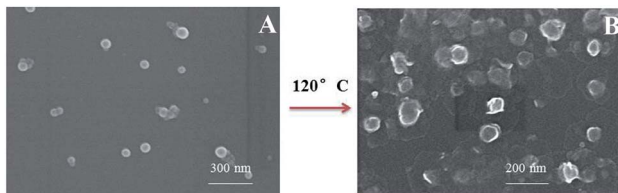


Fig. 9 SEM microscopy of the self-assembled micelles of *iPS-b-1,4-trans-PBD* before (A) and after (B) isothermal crystallization at 150 °C for 3 hours.

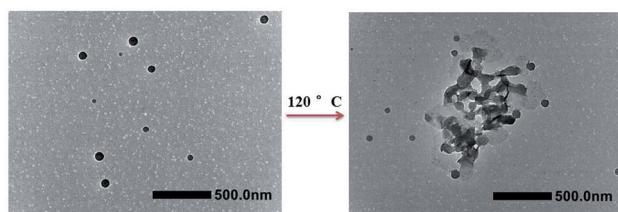


Fig. 10 TEM images of the self-assembled micelles of *iPS-b-1,4-trans-PBD* (Entry 6 in Table 1) before (left) and after (right) isothermal crystallization at 120 °C for 3 hours.

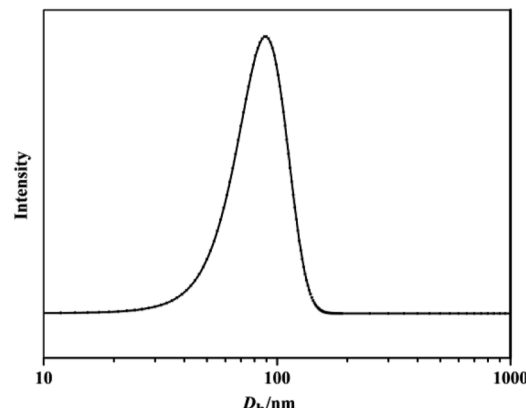


Fig. 11 D_h distributions of the self-assembled micelles of *iPS-b-(1,4-trans-PBD-g-PEO)* prepared from Entry 6 in Table 1 in aqueous solution.

indicating the self-assembly process of the *iPS-b-(1,4-trans-PBD-g-PEO)*. After the THF was completely removed by dialysis against deionized water, the solution was detected by DLS. As exhibited in Fig. 11, the average hydrodynamic diameter (D_h) of the representative self-assembled micelles of *iPS-b-(1,4-trans-*

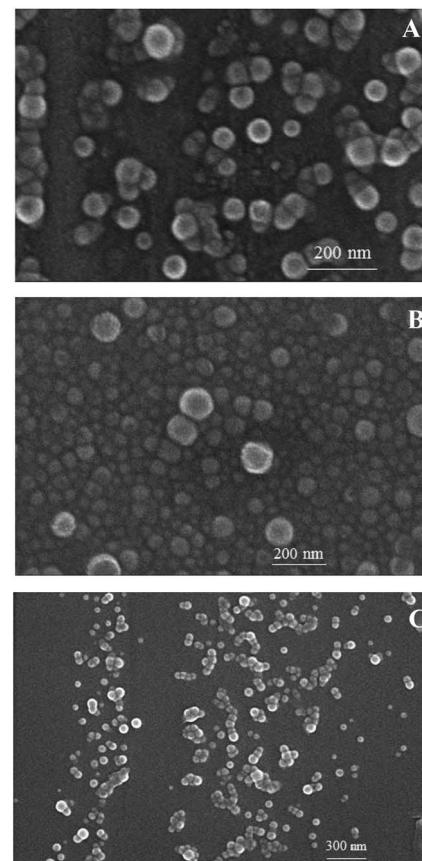


Fig. 12 SEM microscopy of the self-assembled micelles of *iPS-b-(1,4-trans-PBD-g-PEO)* prepared from Entry 6 in Table 1 in aqueous solution after prepared for, respectively, (A). 0 day, (B). 15 day, (C). 30 day.

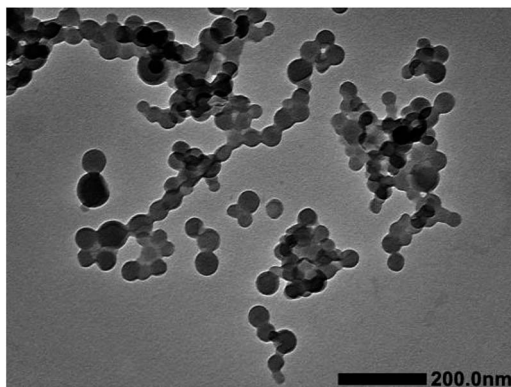


Fig. 13 TEM image of the self-assembled micelles of *iPS-b-(1,4-trans-PBD-g-PEO)* prepared from Entry 6 in Table 1 in aqueous solution.

PBD-g-PEO) prepared from Entry 6 in Table 1 were around 90 nm with narrow distribution, confirming the self-assembling of *iPS-b-(1,4-trans-PBD-g-PEO)* in aqueous solution. In addition, the self-assembled micellar solution was so stable that no obvious precipitation could be observed after prepared for a month. Fig. 12 shows the SEM microscopy of the self-assembled micelles of *iPS-b-(1,4-trans-PBD-g-PEO)* in aqueous solution after prepared for, 0 day, 15 day and 30 day.

Spherical micelles with a diameter of around 70 nm were observed and keep unchanged as time went on. These results were consistent with the DLS detect and its self-assembly behavior was similar to that of *iPS-b-1,4-trans-PBD* in *n*-dodecane, suggesting the formation of an amorphous *iPS* core or with low degree of crystallinity in the micelles as a result of slow crystallization rate of *iPS* and confined crystallization in nano-space. Fig. 13 displays the TEM images of self-assembled micelles of *iPS-b-(1,4-trans-PBD-g-PEO)* in aqueous solution. The uniform round dark domains in the images confirm that spherical micelles but not vesicles were formed and the *iPS* core was amorphous or low crystalline.

Conclusions

iPS-containing diblock copolymers including *iPS-b-1,4-trans-PBD* and a novel amphiphilic diblock copolymer of *iPS-b-(1,4-trans-PBD-g-PEO)* with controlled molecular weight, block ratio and narrow molecular weight distribution were synthesized in terms of living coordination polymerization and graft copolymerization. Moreover, this work also demonstrates the morphology and morphology transition of self-assembled micelles of *iPS-b-1,4-trans-PBD* in *n*-dodecane and *iPS-b-(1,4-trans-PBD-g-PEO)* in aqueous solution. These *iPS*-containing diblock copolymers can all self-assemble into spherical micelles in *n*-dodecane and in aqueous solution, respectively, implying that the core-forming *iPS* block could not crystallize or have a very low degree of crystallinity in nanoconfined space of micelles. It is interesting that heating the micellar solution of *iPS-b-1,4-trans-PBD* in *n*-dodecane to 120 °C and keeping the constant temperature for 3 hours, the micellar morphology changed from sphere-like to platelet-like as a result of the

isothermal crystallization of the core-forming *iPS* block. We suggest that isothermal crystallization would induce the deformation of the micelles.

Conflicts of interest

There are no conflicts to declare.

Acknowledgements

This work was supported by the National Natural Science Foundation of China (21174167, 51573212) and the NSF of Guangdong Province (S2013030013474, 2014A030313178).

Notes and references

- 1 A. Proto, A. Avagliano, D. Saviello, R. Ricciardi and C. Capacchione, *Macromolecules*, 2010, **43**, 5919.
- 2 Z. Y. Li, R. Liu, B. Y. Mai, F. Feng, Q. Wu, G. D. Liang, H. Y. Gao and F. M. Zhu, *Polym. Chem.*, 2013, **4**, 954.
- 3 N. Hadjichristidis, H. Iatou and M. Pitsikalis, *Adv. Polym. Sci.*, 2005, **189**, 1.
- 4 W. Zheng, N. Yan, Y. Zhu, W. Zhao, C. Zhang, H. Zhang, C. Bai, Y. Hu and X. Zhang, *Polym. Chem.*, 2015, **6**, 6088.
- 5 N. Yan, Y. Zhang, Y. He, Y. Zhu and W. Jiang, *Macromolecules*, 2017, **50**, 6771.
- 6 Y. Han, H. Yu, H. Du and W. Jiang, *J. Am. Chem. Soc.*, 2010, **132**, 1144.
- 7 N. Yan, H. Liu, Y. Zhu, W. Jiang and Z. Dong, *Macromolecules*, 2015, **48**, 5980.
- 8 Y. Zhang, Y. He, N. Yan, Y. Zhu and Y. Hu, *J. Phys. Chem. B*, 2017, **121**, 8417.
- 9 M. Wu, Y. Zhu and W. Jiang, *ACS Macro Lett.*, 2016, **5**, 1212.
- 10 Y. He, Y. Zhang, N. Yan, Y. Zhu, W. Jiang and D. Shi, *Nanoscale*, 2017, **9**, 15056.
- 11 W. N. He and J. T. Xu, *Prog. Polym. Sci.*, 2012, **37**, 1350.
- 12 J. Schmelz, F. H. Schacher and H. Schmalz, *Soft Matter*, 2013, **9**, 2101.
- 13 J. J. Crassous, P. Schurtenberger, M. Ballauff and A. M. Mihut, *Polymer*, 2015, **62**, A1.
- 14 A. M. Mihut, J. J. Crassous, H. Schmalz, M. Drechsler and M. Ballauff, *Soft Matter*, 2012, **8**, 3163.
- 15 J. Raez, J. P. Tomba, I. Manners and M. A. Winnik, *J. Am. Chem. Soc.*, 2003, **125**, 9546.
- 16 J. Raez, I. Manners and M. A. Winnik, *Langmuir*, 2002, **18**, 7229.
- 17 S. F. M. Yusoff, J. B. Gilroy, G. Cambridge, M. A. Winnik and I. Manners, *J. Am. Chem. Soc.*, 2011, **133**, 11220.
- 18 E. K. Lin and A. P. Gast, *Macromolecules*, 1996, **29**, 4432.
- 19 H. Schmalz, J. Schmelz, M. Drechsler, J. Yuan, A. Walther, K. Schweimer and A. M. Mihut, *Macromolecules*, 2008, **41**, 3235.
- 20 T. Li, W. J. Wang, R. Liu, W. H. Liang, G. F. Zhao, Z. Y. Li, Q. Wu and F. M. Zhu, *Macromolecules*, 2009, **42**, 3804.
- 21 R. Liu, Z. Y. Li, B. Y. Mai, Q. Wu, G. D. Liang, H. Y. Gao and F. M. Zhu, *J. Polym. Res.*, 2013, **20**, 64.



22 A. Radulescu, R. T. Mathers, G. W. Coates, D. Richter and L. J. Fetter, *Macromolecules*, 2004, **7**, 6962.

23 J. Massey, K. N. Power, I. Manners and M. A. Winnik, *J. Am. Chem. Soc.*, 1998, **20**, 9533.

24 G. Guerin, J. Raez, I. Manners and M. A. Winnik, *Macromolecules*, 2005, **38**, 7819.

25 X. S. Wang, K. Liu, A. C. Arsenault, D. A. Rider, G. A. Ozin, M. A. Winnik and I. Manners, *J. Am. Chem. Soc.*, 2007, **129**, 5630.

26 J. T. Xu, J. P. A. Fairclough, S. M. Mai and A. J. Ryan, *J. Mater. Chem.*, 2003, **13**, 2740.

27 J. T. Xu, G. D. Liang, S. M. Mai and A. J. Ryan, *Chem. J. Chin. Univ.*, 2004, **25**, 1978.

28 A. M. Mihut, M. Drechsler, M. Moller and M. Ballauff, *Macromol. Rapid Commun.*, 2010, **31**, 449.

29 D. Portinha, F. Boue, L. Bouteiller, G. Carrot, C. Chassenieux, S. Pensec and G. Reiter, *Macromolecules*, 2007, **40**, 4037.

30 J. Fu, B. Luan, X. Yu, Y. Cong, J. Li, C. Y. Pan, Y. C. Han, Y. M. Yang and B. Y. Li, *Macromolecules*, 2004, **37**, 976.

31 K. Rajagopal, A. Mahmud, D. A. Christian, J. D. Pajerowski, A. E. X. Brown, S. M. Loverde and D. E. Discher, *Macromolecules*, 2010, **43**, 9736.

32 Z. X. Du, J. T. Xu and Z. Q. Fan, *Macromolecules*, 2007, **40**, 7633.

33 Z. X. Du, J. T. Xu and Z. Q. Fan, *Macromol. Rapid Commun.*, 2008, **29**, 467.

34 W. N. He, J. T. Xu, B. Y. Du, Z. Q. Fan and X. S. Wang, *Macromol. Chem. Phys.*, 2010, **211**, 1909.

35 S. C. Chan, S. W. Kuo, C. H. Lu, H. F. Lee and F. C. Chang, *Polymer*, 2007, **48**, 5059.

36 Z. C. Li, R. J. Ono, Z. Q. Wu and C. W. Bielawski, *Chem. Commun.*, 2011, **47**, 197.

37 A. C. Kamps, M. Fryd and S. J. Park, *ACS Nano*, 2012, **6**, 2844.

38 M. Lazzari, D. Scalarone, C. E. Hoppe, C. Vazquez-Vazquez and M. A. Lopez-Quintela, *Chem. Mater.*, 2007, **19**, 5818.

39 M. Lazzari, D. Scalarone, C. Vazquez-Vazquez and M. A. Lopez-Quintela, *Macromol. Rapid Commun.*, 2008, **29**, 352.

40 G. Natta, P. Corradini and I. W. Bassi, *Nuovo Cimento*, 1960, **15**, 68.

41 P. J. Lemstra and G. Challa, *J. Polym. Sci., Part B: Polym. Lett.*, 1975, **13**, 1809.

42 P. J. Lemstra, J. Postma and G. Challa, *Polymer*, 1974, **15**, 757.

43 G. Xue, Y. Wang, X. Gu and Y. Lu, *Macromolecules*, 1994, **27**, 4016.

44 C. Capacchione, A. Proto, H. Ebeling, R. Mulhaupt, K. Moller, T. P. Spaniol and J. Okuda, *J. Am. Chem. Soc.*, 2003, **125**, 4964.

45 K. Beckerle, R. Manivannan, T. P. Spaniol and J. Okuda, *Organometallics*, 2006, **25**, 3019.

46 C. Capacchione, R. Manivannan, M. Barone, K. Beckerle, R. Centore, L. Oliva, A. Proto, A. Tuzi, T. P. Spaniol and J. Okuda, *Organometallics*, 2005, **24**, 2971.

47 A. Rodrigues, E. Kirillov, T. Roisnel, A. Razavi, B. Vuillemin and J. F. Carpentier, *Angew. Chem., Int. Ed.*, 2007, **46**, 7240.

48 T. Kawasaki, C. Hohberger, Y. Araki, K. Hatase, K. Beckerle, J. Okuda and K. Soai, *Chem. Commun.*, 2009, 5621.

49 T. C. Chung, M. Raate, M. Berluche and D. M. Schulz, *Macromolecules*, 1988, **21**, 1903.

50 S. Ramakrishnan, *Macromolecules*, 1991, **24**, 3753.

